

A rabbit femoral trochlear defect model for chondral and osteochondral regeneration

Tung Nguyen-Thanh^{1,2}, Bao-Song Nguyen-Tran³, Sara Cruciani⁴,
Thuan Dang-Cong³, Margherita Maioli⁴

¹Hue University, University of Medicine and Pharmacy, Faculty of Basic Science, Hue, Vietnam

²Hue University, University of Medicine and Pharmacy, Institute of Biomedicine, Hue, Vietnam

³Hue University, University of Medicine and Pharmacy, Department of Histology, Embryology, Pathology and Forensic, Hue, Vietnam

⁴University of Sassari, Department of Biomedical Sciences, Sassari, Italy

Received December 7, 2021

Accepted June 14, 2022

Abstract

Articular cartilage degeneration represents one of the main features of osteoarthritis. Recently, novel approaches based on biomaterials have been successfully applied to osteochondral regeneration. Our study was carried out on rabbits to assess a model of articular cartilage damage to test biomaterials for osteochondral regeneration. We created osteochondral defects on the surface of the trochlear groove area of the femurs in 15 white male New Zealand rabbits of the size of 3 mm × 3 mm (diameter × depth). Rabbits were then monitored and samples were collected 2 weeks, 4 weeks, and 6 weeks after the operation. The reconstruction of defects was assessed macroscopically according to the International Cartilage Repair Society (ICRS) scale and radiography (X-ray). For microscopic evaluation, haematoxylin-eosin staining and safranin O staining were used. The defects were repaired by regenerative tissue, and the recovery results gradually increased after 2 weeks, 4 weeks, and 6 weeks, showing both microscopically and macroscopically. However, the regenerative tissue was mainly fibrous connective tissue, not cartilage or bone. This is a model of articular cartilage damage that is suitable for early screening of preclinical studies related to osteochondral regeneration using biomaterials.

Regenerative medicine, cartilage regeneration, bone regeneration, animal models, osteochondral regeneration

Osteoarthritis is the most common form of arthritis, which involves mainly load-bearing joints such as knees and hips, affecting millions of people worldwide. It is featured by the degeneration and changes of the articular cartilage as well as the subchondral bone layer (Wang et al. 2011). Because of the shortage of blood vessels, nerves, and lymphatics, articular cartilage's ability to self-renew and recover after an injury is very limited (Huey et al. 2012). Treatment of osteoarthritis is often persistent and ineffective, mainly based on symptomatic treatment with analgesics, anti-inflammatory drugs, and physical therapy. Moreover, in severely affected patients total joint arthroplasty is needed, involving higher sanitary costs as well as risks of complications after surgery (Kristjánsson and Honsawek 2014; Park et al. 2017). In recent years, methods for applying biomaterials in osteochondral regeneration have been studied and shown to be effective. It is compulsory to perform *in vivo* studies on animals to assess the safety, feasibility, and effectiveness of new interventional treatments before clinical trials. For a study of applying biomaterials in osteochondral regeneration, the selection of an experimental animal model is very important and depends on many factors such as similarities in anatomical and physiological

Addresses for correspondence:

Tung Nguyen-Thanh
Institute of Biomedicine
University of Medicine and Pharmacy, Hue University
6 Ngo Quyen Street, Hue 49000, Vietnam

E-mail: nguyenthanhtung@hueuni.edu.vn;
nttung@huemed-univ.edu.vn

Margherita Maioli
Department of Biomedical Sciences
University of Sassari
Viale San Pietro 43/B, 07100 Sassari, Italy

E-mail: mmaioli@uniss.it
<http://actavet.vfu.cz/>

characteristics to humans, cost-effectiveness, care time, and medical ethics issues. The animals that are often selected include mice, rabbits, dogs, goats, pigs, sheep, etc., of which rabbits are very suitable subjects in short-term evaluation experiments (Chu et al. 2010; Cook et al. 2014; Meng et al. 2020).

Our study was carried out to evaluate a model of articular cartilage damage in rabbits in order to build an optimal model for osteochondral regeneration experiments in this species.

Materials and Methods

Animals

A total of 15 adult male white rabbits of the New Zealand breed, weighing 2.3–2.5 kg were used in our study following the standardized procedure which was approved by the Animal Ethics Committee of the Hue University (Certificate No. HUVN0010). The animals were kept in separate cages and were given pellet feed and tap water. They were divided into 5 groups: Control ($n = 3$); First day of defect induction (D0, $n = 3$); 2 weeks after inducing defects (2W, $n = 3$); 4 weeks after inducing defects (4W, $n = 3$); and 6 weeks after inducing defects (6W, $n = 3$).

Study design

Surgical procedures

Anaesthesia was induced by an intramuscular injection of 40 mg/kg ketamine hydrochloride (Troy laboratories, Sydney, Australia) and 5 mg/kg xylazine hydrochloride (Troy laboratories, Sydney, Australia). In sterile conditions, a medial peripatellar incision was made in the knee of the right posterior limb of each rabbit, and the patella was dislocated laterally. After that, an osteochondral defect with 3 mm in diameter and 3 mm in depth was created on the trochlear groove of the femur by using a biopsy punch to navigate the site and the size, then a dental stainless drill was used to induce the interest defect (Plate XVI, Fig. 1).

Rabbits were injected with the antibiotic gentamicin 4 mg/kg (Hanvet Co., Ltd., Hung Yen, Vietnam), subcutaneously for 3 consecutive days after surgery to avoid wound infection. The rabbits were nursed in separate cages, checked, and assessed for the condition of the incision as well as the general condition daily.

Sample collection

At 2 weeks, 4 weeks, and 6 weeks after surgical operation, rabbits were sacrificed, and the distal ends of the femurs containing defects were collected. For group D0, we created the defects and then collected samples on the same day as for group 6W. For the control group, which was left without induction of defects, we collected samples on the same day as for group 6W. All samples were assessed macroscopically, radiographed, and histologically analyzed.

Gross morphology

The distal parts of the femurs were excised, photographed, and graded for cartilaginous regeneration by the International Cartilage Repair Society (ICRS) macroscopic assessment score (Table 1).

Radiography assessment

After 2, 4, and 6 weeks, distal parts of the femurs were collected and evaluated by the EZDent X-ray machine (Vatech Co., Ltd., Gyeonggi-do, Korea). Root X-ray film was placed at the lateral position of the surgical defect and recorded with a current of 65 kvp, 7.5 mA for 0.25 s. X-ray images were analyzed using EZDent biomedical software (Vatech Co., Ltd., Gyeonggi-do, Korea).

Haematoxylin-eosin stain and safranin O

Each tissue sample was fixed in 10% neutral formal for 48 h and then immersed in 10% EDTA solution (Sigma-Aldrich, Darmstadt, Germany) for 8 weeks to decalcify. After 8 weeks of decalcification, the tissue samples were cut into small pieces of the size of $1.0 \times 1.0 \times 0.5$ cm (length \times width \times thickness) each. The sample containing the defect was taken for tissue processing, paraffin embedding, and sectioning into 3- μ m slices to stick on the slide. These samples were stained with haematoxylin-eosin (Sigma-Aldrich) for the overall assessment of the tissue and 0.25% safranin O (Sigma-Aldrich) for histologic evaluation of cartilage tissue renewal.

Microscopic assessment

Cartilaginous regeneration was assessed histologically according to the scale of Wakitani (Wakitani et al. 1994). The evaluation categories include cell morphology, matrix-staining, surface regularity, thickness of the cartilage and integration of the donor cartilage with the host adjacent cartilage (Table 2).

Statistical analysis

Results were analyzed using Predictive Analytics SoftWare (PASW) statistic 18 (SPSS Inc, Chicago, IL). All data were reported as mean \pm standard deviation (SD). For evaluation of significant differences, the comparison of means between two experimental groups was analyzed using nonparametric Mann-Whitney U test. Differences were considered to be significant at $P \leq 0.05$.

Table 1. Macroscopic assessment according to the Internal Cartilage Repair Society score

| Category | Score |
|---|-------|
| Degree of defect repair | |
| in level with surrounding cartilage | 4 |
| 75% repair of defect depth | 3 |
| 50% repair of defect depth | 2 |
| 25% repair of defect depth | 1 |
| 0% repair of defect depth | 0 |
| Integration to the border zone | |
| complete integration with surrounding cartilage | 4 |
| demarcating border <1 mm | 3 |
| 3/4 of graft integrated, 1/4 with a notable border >1 mm width | 2 |
| 1/2 of graft integrated with surrounding cartilage, 1/2 with a notable border >1 mm | 1 |
| from no contact to 1/4 of graft integrated with surrounding cartilage | 0 |
| Macroscopic appearance | |
| intact smooth surface | 4 |
| fibrillated surface | 3 |
| small, scattered fissures or cracks | 2 |
| several, small or few but large fissures | 1 |
| total degeneration of the grafted area | 0 |
| Overall repair assessment | |
| Grade I: Normal | 12 |
| Grade II: Nearly normal | 8-11 |
| Grade III: abnormal | 4-7 |
| Grade IV: Severely abnormal | 1-3 |

Results

Macroscopic assessment of osteochondral defect repair and ICRS score

The results of macroscopic observations are presented in Fig. 2a-e, and ICRS macroscopic assessment scores are presented in Fig. 2f (Plate XVII). Two weeks after the operation, the bottoms of the defects were filled with pinkish-white soft tissue, 2 mm from the mouth of the defects, and their diameters were partially narrowed. After 4 weeks, the bottoms of the defects were filled with pinkish-white soft tissue, their diameters were narrower compared to the 2-week group. In the 6-week group, the defects were filled about 50%, and the surfaces of the defects were relatively smooth. Evaluation results according to the ICRS scale showed that cartilage defects were partially regenerated after 2, 4, and 6 weeks of induction. Normal articular cartilage is rated 12 points. The average ICRS score at 4 weeks (3.67 ± 0.58) was higher than that at 2 weeks (2.33 ± 0.58), but this difference was not significant. However, after 6 weeks, the average ICRS score became significant compared to what was observed after 4 and 2 weeks (5.33 ± 0.58) (Plate XVII, Fig. 2f).

Assessment of subchondral bone formation by radiography

The radiographic evaluation of subchondral bone formation is presented in Fig. 3 (Plate XVIII). The radiographic image of a normal rabbit femoral head is shown in Fig. 3b. The defect model produces a well-defined bone resorption image. After 2 weeks, the borderline is not clearly defined, suggesting the possibility of peripheral osteogenesis. After 4 and

Table 2. Wakitani histological scale for cartilaginous regeneration (Wakitani et al. 1994).

| Category | Score |
|---|-------|
| Cell morphology | |
| hyaline cartilage | 0 |
| mostly hyaline cartilage | 1 |
| mostly fibrocartilage | 2 |
| mostly non-cartilage | 3 |
| non-cartilage only | 4 |
| Matrix staining (metachromasia) | |
| normal (compared with host adjacent cartilage) | 0 |
| slightly reduced | 1 |
| markedly reduced | 2 |
| no metachromatic stain | 3 |
| Surface regularity | |
| smooth ($> 3/4$) | 0 |
| moderate ($> 1/2 - 3/4$) | 1 |
| irregular ($1/4 - 1/2$) | 2 |
| severely irregular ($< 1/4$) | 3 |
| Thickness of cartilage | |
| $> 2/3$ | 0 |
| $1/3 - 2/3$ | 1 |
| $< 1/3$ | 2 |
| Integration of the donor cartilage with the host adjacent cartilage | |
| both edges integrated | 0 |
| one edges integrated | 1 |
| neither edge integrated | 2 |
| Total maximum | 14 |

6 weeks, the area of bone resorption gradually decreases and is replaced by cancellous trabeculae. The bone density is still not normal, but there is a reconstructed trabecular structure similar to the image of osteoporosis.

Histological assessment and Wakitani scale

The histological assessment results of the osteochondral defect regeneration are presented in Figs 4 and 5. Samples from rabbits of the control group exhibited the typical structure of the articular cartilage in the knee joint, including hyaline cartilage (HC), superficial zone (SZ), middle zone (MZ), deep zone (DZ), calcified zone (CZ), subchondral bone (SB), bone marrow cavity (BMC), chondrocytes (asterisk) and osteocytes (arrowhead). The surgery created a hole from the outermost area of the hyaline cartilage to the subchondral bone area. Two weeks post surgery, the defect was filled with fibrous connective tissue, with fibroblast cells intermingled in the matrix at a relatively high density. After 4 weeks, the fibrous connective tissue became thinner, the underlying layer showed a proliferation of fat niches, and bone marrow cells were interspersed in the bone trabeculae. On the surface of the defect near the site of normal tissue, chondrocytes and cartilage matrix appeared. After 6 weeks, the remaining fibrous connective tissue was much thinner than in

the 4-week group. The presence of renewal cartilage tissue and ossified bone was slightly more apparent than in the 4-week group, although it was still scattered and discontinuous. Below the surface layer, the fibrous connective tissue was replaced by fat niches and bone marrow cells located in the bone trabeculae (Plate XIX, Fig. 4).

The staining of cartilage matrix with safranin O is shown in Fig. 5a-d (Plate XX). The results showed that the cartilaginous tissue and the calcified zone were orange whereas the subchondral bone was pink, and the connective tissue was red. After 2 weeks, the defect area was mostly filled with fibrous connective tissue. After 4 and 6 weeks, cartilage tissue began to form. Especially, after 6 weeks, cartilage tissue formed scattered in the middle of the defect area.

According to the histological scale for cartilaginous regeneration of Wakitani et al. (1994), the normal cartilage tissue is scored 0. After 2 weeks of surgery, the average score of the lesion was high (11.33 ± 1.15). After 4 and 6 weeks, the lesion's score decreased significantly (8.33 ± 0.58 and 6.67 ± 0.58) (Plate XX, Fig. 5e)

Discussion

Small animals, such as rats, mice, guinea pigs, and rabbits represent the commonly employed animal models to study cartilage regeneration (77%). These animals have the advantages of low cost, easy experimental procedures, as well as care and monitoring. However, they have their limitations, such as small joint size, thin cartilage layer (it ranges within 0.03–0.4 mm and 0.2–0.7 mm in mice and rabbits, respectively, whereas in humans it ranges within 2.2–2.5 mm), and the spontaneous healing ability (Chu et al. 2010; McCoy 2015; Meng et al. 2020). These small animals are suitable for pathogenesis experiments and preclinical trials for new therapies. Other animal models for the study of cartilage regeneration include large animals, such as goats, dogs, pigs, sheeps, and horses. The advantage of these species is that the anatomical structure of the joint (alveolar size, cartilage thickness) and clinical lesions are similar to those of humans. However, the disadvantages of these large animal models are the high cost, problems in performing experiments, in care, and the high ethical concerns (Chu et al. 2010; McCoy 2015; Meng et al. 2020). They are often used in studies to test new therapies, especially materials for the treatment of osteochondral regeneration.

Osteoarthritis is a common chronic degenerative joint disease involving mainly load-bearing joints such as the knees and hips. In studies on animal models, the knee joint is often chosen to do experiments on, as it is easier to manage than the hip joint. There are several methods to create an articular cartilage damage model, including the injection of a cytotoxic agent, destabilization of the joint, and inducing osteochondral defects as the most common method (Table 3).

Bove et al. (2003) studied the effects of load-bearing changes in osteoarthritis progression and the effect of anti-inflammatory agents in its treatment in rats by injecting 1 mg of mono-iodoacetate (MIA) into the knee joint. Histopathological results (haematoxylin-eosin and toluidin blue staining) showed that after 7 days, there was a loss of chondrocytes with degeneration of proteoglycan (cartilage matrix). After 14 days, the chondrocytes and proteoglycan matrix in the deeper part also disappeared and the lesion spread to 2/3 of the tibial plateau (Bove et al. 2003). In 2007, Ivanavicius et al. (2007) set up a similar model of joint damage while studying the mechanism of peripheral nerve damage in osteoarthritis. Microscopic results (haematoxylin-eosin staining) showed that after 8 days of MIA injection, the structure of both articular cartilage layer and subchondral bone degeneration was induced. The damage was more evident after 12, 14, 21 days and after 28 days: the cartilage tissue, as well as subchondral bone disappeared and the cancellous bone underneath was also remodeled (Ivanavicius et al. 2007). Other researchers applied

Table 3. Studies of creating cartilage defects on animal models.

| Authors | Species | Location | Defect size (diameter × depth) |
|---------------------------|---------|-----------------------------------|-----------------------------------|
| Dahlin et al. (2014) | Rat | The trochlear groove of the femur | 2 mm × 2 mm |
| Huade et al. (2009) | Rat | The trochlear groove of the femur | 1.5 mm × 2 mm |
| Schlichting et al. (2008) | Sheep | The femoral condyles | 7.3 mm × 10 mm |
| Kazemi et al. (2017) | Dog | The medial femoral condyles | 6 mm × 5 mm |
| Kon et al. (2015) | Goat | The medial femoral condyles | 6 mm × 10 mm |
| McCarrel et al. (2017) | Horse | The lateral femoral condyles | 10 mm × 10 mm |
| Katayama et al. (2004) | Rabbit | The trochlear groove of the femur | 4 mm × 4 mm |
| Liao et al. (2015) | Rabbit | The trochlear groove of the femur | 4 mm × 3 mm |
| Frenkel et al. (2005) | Rabbit | The medial femoral condyles | 3 mm × 2.8 mm |
| Zhu et al. (2017) | Rabbit | The medial femoral condyles | 4.5 mm × 4.5 mm |
| This study | Rabbit | The trochlear groove of the femur | 3 mm × 3 mm |

the same method to rats or mice (Clements et al. 2009; Pitcher et al. 2016). These studies showed that MIA injection in rat knee joints caused articular cartilage damage with histopathological features similar to osteoarthritis in humans. However, the time to induce damage was quite long. This model was commonly used to determine the pathogenesis and evaluate the effects of pharmacological agents in protecting the cartilage structure.

Another method of creating articular cartilage damage is causing destabilization of the joint. In 2003, Murphy et al. (2003) performed experiments on goats by completely removing the medial meniscus along with resecting the anterior cruciate ligament of the knee joint, then injecting autologous stem cells to evaluate the effectiveness of cell therapy in osteoarthritis. The results showed that this method generated typical lesions in osteoarthritis including erosive damage to articular cartilage in the ends of the femur and the tibial plateau; production of osteophytes, and changes in the subchondral trabecular structure, appearing 6 weeks after surgery (Murphy et al. 2003). In 2004, Batiste et al. (2004) used a similar method in rabbits. After 4, 8, and 12 weeks, erosive articular cartilage lesions appeared at both the tibia plateau and the end of the femur, progressing worse over experiment time. The slow progression of articular cartilage lesions produced by this method is suitable for pharmaceutical studies (Samvelyan et al. 2020).

In 2007, Glasson et al. (2007) used the method of resecting the middle meniscus ligament causing instability of the meniscus in the knee joint of transgenic mice 129/SvEv. After 8 weeks of surgery, cartilage erosion occurred in both femoral condyles and the tibial plateau (Glasson et al. 2007). Ma et al. (2007) also used the same method to create a model of articular cartilage damage in 129S6/SvEv transgenic mice, aiming at evaluating the role of sex hormones in cartilage degeneration and progression of osteoarthritis (Ma et al. 2007). This model has been used for targeted validation research using transgenic animals to evaluate the pathophysiological roles of different molecules and enzymes in osteoarthritis (Samvelyan et al. 2020).

The method of creating articular cartilage defects is the most common, simulating the damage that occurs after a severe collision, sports injury, or physical disease leading to joint pain, destruction, and loss of joint function (Deng et al. 2019). This method is applied to many different animal species, from small-sized species to large-sized species. Cartilage defect models are widely used in preclinical studies of new treatments, especially cartilage-regenerating materials, thanks to the faster creation of cartilage damage, and the chance to test materials directly into the lesion. The selection of animals to perform the cartilage defect model should take into account the joint size, cartilage thickness, depth and diameter

of the defect, age of skeletal maturity, cost, and the possibility of care and follow-up in the animals (Cook et al. 2014; McCoy et al. 2015; Meng et al. 2020).

In our study, we used the New Zealand white rabbit, being the most suitable subject for our implementation conditions with the following advantages: acceptable cost, surgical conditions not complicated, easy to care for, follow up after surgery, and do not face major ethical issues like other large animals.

Osteochondral defects of the knee joint can be created on the trochlear groove or femoral condyles (Table 3). The joints of experimental animals are often subjected to maximum weight-bearing as normal immediately after surgery, and therefore the trochlear groove was chosen for a better protection of the grafting materials since it is less weight-bearing than the femoral condyles (Ahern et al. 2009). In addition, results of several studies showed that the healing of defects of the trochlear groove was better than that of the femoral condyles (Evans et al. 2009; Chen et al. 2013).

It is very important to consider the “critical diameter” of the defect. This is the size necessary to limit the natural regenerative capability of the cartilage, which can lead to an unbiased assessment of the effectiveness of the grafting materials (Table 3) (Colman et al. 1999; Malda et al. 2013; Moran et al. 2016; Meng et al. 2020). We created defects on the trochlear groove of the rabbit knee joint of the size of 3 mm in diameter and 3 mm in depth. According to previous studies, 3 mm is the critical diameter of the cartilage defect in the experimental rabbit model (Table 4).

Table 4. Differences in skeletal maturity, cartilage feature, and defect size in model animals (Colman et al. 1999; Malda et al. 2013; Moran et al. 2016).

| Species | Skeletal maturity (age) | Cartilage thickness | Critical diameter of defects | Depth of defects |
|---------|-------------------------|---------------------|------------------------------|------------------|
| Rat | 7 months | 0.10 mm | 1.4 mm | 1.0–2.0 mm |
| Rabbit | 9 months | 0.30 mm | 3.0 mm | 3.0–5.0 mm |
| Dog | 12–24 months | 0.95 mm | 4.0 mm | 10–12 mm |
| Pig | 18 months | 1.50 mm | 6.3 mm | 8–10 mm |
| Sheep | 2–3 years | 0.45 mm | 7.0 mm | 6–13 mm |
| Goat | 2–3 years | 1.10 mm | 6.0 mm | 6–12 mm |
| Horse | 2–4 years | 1.75 mm | 4.0 mm/9 mm | 10 mm |
| Human | 18–22 years | 2.35 mm | - | - |

To evaluate the cartilage regeneration of the defects, we used the International Society of Cartilage Regeneration (ICRS) macroscopic scale and the microscopic scale of Wakitani (based on the histological images stained with haematoxylin-eosin and safranin O) (Wakitani et al. 1994). These are common methods used in studies involving cartilaginous regeneration in experimental animal models. In addition, we also used x-ray to evaluate the subchondral bone formation during this regenerative process. The results demonstrated that the defects were repaired by regenerative tissue, and the recovery results gradually increased after 2, 4, and 6 weeks, demonstrated both microscopically and macroscopically. However, the regenerative tissue was mainly fibrous connective tissue; cartilage tissue and ossified bone were formed scattered after 4 and 6 weeks. This result proves that the size of the defects in our study was appropriate, limiting the ability of spontaneous regeneration of osteochondral tissue of experimental rabbits.

However, our model still exhibits limitations. Recent studies recommend a larger diameter of 4–5 mm to completely exclude the self-healing ability of rabbits, in order to increase the accuracy of evaluating the effectiveness of grafting materials (Katayama et al. 2004; McCoy et al. 2015; Zhu et al. 2017). However, in our study, the diameter

of the defect was 3 mm, being the “optimal diameter” in the experimental rabbit model. Another limitation of our study is the duration. Our study lasted 6 weeks, which is quite short compared to other studies. The follow-up time for articular cartilage regeneration in many studies on experimental rabbit models lasted 8 to 12 weeks, or longer (24 weeks) (Katayama et al. 2004; Liao et al. 2015; Zhu et al. 2017). The experimental time in these studies was longer partly due to the larger defect size (diameter of 4–4.5 mm), which took longer to recover.

In conclusion, our study established a model of articular cartilage damage in rabbits with the following advantages: low cost, uncomplicated surgical conditions, easy care, easy follow-up after surgery, and no major ethical issues. Besides, this model has some issues to be improved such as increasing the size of the defect and prolonging the time of the experiment. This model is suitable for studies to initially evaluate the effectiveness of interventional therapies for articular cartilage lesions, especially implantable materials.

Acknowledgements

This study was supported by the Vietnamese Ministry of Education and Training’s research projects in science and technology (B2020-DHH-12). The authors also acknowledge the partial support of Hue University under the Core Research Program (NCM.DHH.2022.02).

References

- Ahern BJ, Parvizi J, Boston R, Schaer TP 2009: Preclinical animal models in single site cartilage defect testing: a systematic review. *Osteoarthritis Cartilage* **17**: 705-713
- Batiste DL, Kirkley A, Laverty S, Thain LM, Spouge AR, Holdsworth DW 2004: *Ex vivo* characterization of articular cartilage and bone lesions in a rabbit ACL transection model of osteoarthritis using MRI and micro-CT. *Osteoarthritis Cartilage* **12**: 986-996
- Bove SE, Calcaterra SL, Brooker RM, Huber CM, Guzman RE, Juneau PL, Schrier DJ, Kilgore KS 2003: Weight bearing as a measure of disease progression and efficacy of anti-inflammatory compounds in a model of monosodium iodoacetate-induced osteoarthritis. *Osteoarthritis Cartilage* **11**: 821-830
- Chen H, Chevrier A, Hoemann CD, Sun J, Picard G, Buschmann MD 2013: Bone marrow stimulation of the medial femoral condyle produces inferior cartilage and bone repair compared to the trochlea in a rabbit surgical model. *J Orthop Res* **31**: 1757-1764
- Chu CR, Szczodry M, Bruno S 2010: Animal models for cartilage regeneration and repair. *Tissue Eng Part B Rev* **16**: 105-115
- Clements KM, Ball AD, Jones HB, Brinckmann S, Read SJ, Murray F 2009: Cellular and histopathological changes in the infrapatellar fat pad in the monoiodoacetate model of osteoarthritis pain. *Osteoarthritis Cartilage* **17**: 805-812
- Colman RJ, Lane MA, Binkley N, Wegner FH, Kemnitz JW 1999: Skeletal effects of aging in male rhesus monkeys. *Bone* **24**: 17-23
- Cook JL, Hung CT, Kuroki K, Stoker AM, Cook CR, Pfeiffer FM, Sherman SL, Stannard JP 2014: Animal models of cartilage repair. *Bone Jt Res* **3**: 89-94
- Dahlin RL, Kinard LA, Lam J, Needham CJ, Lu S, Kasper FK, Mikos AG 2014: Articular chondrocytes and mesenchymal stem cells seeded on biodegradable scaffolds for the repair of cartilage in a rat osteochondral defect model. *Biomaterials* **35**: 7460-7469
- Deng C, Chang J, Wu C 2019: Bioactive scaffolds for osteochondral regeneration. *J Orthop Translat* **17**: 15-25
- Evans CH, Liu FJ, Glatt V, Hoyland JA, Kirker-Head C, Walsh A, Betz O, Wells JW, Betz V, Porter RM, Saad FA, Gerstenfeld LC, Einhorn TA, Harris MB, Vrahas MS 2009: Use of genetically modified muscle and fat grafts to repair defects in bone and cartilage. *Eur Cells Mater* **18**: 96-111
- Frenkel SR, Bradica G, Brekke JH, Goldman SM, Ieska K, Issack P, Bong MR, Tian H, Gokhale J, Coutts RD, Kronengold RT 2005: Regeneration of articular cartilage – Evaluation of osteochondral defect repair in the rabbit using multiphasic implants. *Osteoarthritis Cartilage* **13**: 798-807
- Glasson SS, Blanchet TJ, Morris EA 2007: The surgical destabilization of the medial meniscus (DMM) model of osteoarthritis in the 129/SvEv mouse. *Osteoarthritis Cartilage* **15**: 1061-1069
- Huade L, Qiang Z, Yuxiang X, Jie F, Zhongli S, Zhijun P 2009: Rat cartilage repair using nanophase PLGA/HA composite and mesenchymal stem cells. *J Bioact Compat Polym* **24**: 83-99
- Huey DJ, Hu JC, Athanasias KA 2012: Unlike bone, cartilage regeneration remains elusive. *Science (New York, NY)* **338**: 917-921
- Ivanavicius SP, Ball AD, Heapy CG, Westwood RF, Murray F, Read SJ 2007: Structural pathology in a rodent model of osteoarthritis is associated with neuropathic pain: increased expression of ATF-3 and pharmacological characterisation. *Pain* **128**: 272-282

- Katayama R, Wakitani S, Tsumaki N, Morita Y, Matsushita I, Gejo R, Kimura T 2004: Repair of articular cartilage defects in rabbits using CDMPI gene-transfected autologous mesenchymal cells derived from bone marrow. *Rheumatology* **43**: 980-985
- Kazemi D, Shams Asenjan K, Dehdilani N, Parsa H 2017: Canine articular cartilage regeneration using mesenchymal stem cells seeded on platelet rich fibrin: Macroscopic and histological assessments. *Bone Jt Res* **6**: 98-107
- Kristjánsson B, Honsawek S 2014: Current perspectives in mesenchymal stem cell therapies for osteoarthritis. *Stem Cells Int* **2014**: 194318
- Kon E, Filardo G, Shani J, Altschuler N, Levy A, Zaslav K, Eisman JE, Robinson D 2015: Osteochondral regeneration with a novel aragonite-hyaluronate biphasic scaffold: up to 12-month follow-up study in a goat model. *J Orthop Surg Res* **10**: 81-81
- Liao J, Qu Y, Chu B, Zhang X, Qian Z 2015: Biodegradable CSMA/PECA/graphene porous hybrid scaffold for cartilage tissue engineering. *Sci Rep* **5**: 9879-9879
- Ma HL, Blanchet TJ, Peluso D, Hopkins B, Morris EA, Glasson SS 2007: Osteoarthritis severity is sex dependent in a surgical mouse model. *Osteoarthr Cartil* **15**: 695-700
- Malda J, de Grauw J, Benders K, Kik M, Lest C, Creemers L, Dhert W, van Weeren P 2013: Of mice, men and elephants: The relation between articular cartilage thickness and body mass. *PloS One* **8**: e57683
- McCarrel TM, Pownder SL, Gilbert S, Koff MF, Castiglione E, Saska RA, Bradica G, Fortier LA 2017: Two-year evaluation of osteochondral repair with a novel biphasic graft saturated in bone marrow in an equine model cartilage **8**: 406-416
- McCoy AM 2015: Animal models of osteoarthritis: Comparisons and key considerations. *Vet Pathol* **52**: 803-818
- Meng X, Ziadlou R, Grad S, Alini M, Wen C, Lai Y, Qin L, Zhao Y, Wang X 2020: Animal models of osteochondral defect for testing biomaterials. *Biochem Res Int* **2020**: 9659412
- Moran CJ, Ramesh A, Brama PA, O'Byrne JM, O'Brien FJ, Levingstone TJ 2016: The benefits and limitations of animal models for translational research in cartilage repair. *J Exp Orthop* **3**: 1
- Murphy JM, Fink DJ, Hunziker EB, Barry FP 2003: Stem cell therapy in a caprine model of osteoarthritis. *Arthritis Rheum* **48**: 3464-3474
- Park YB, Ha CW, Lee CH, Yoon YC, Park YG 2017: Cartilage regeneration in osteoarthritic patients by a composite of allogeneic umbilical cord blood-derived mesenchymal stem cells and hyaluronate hydrogel: results from a clinical trial for safety and proof-of-concept with 7 years of extended follow-up. *Stem Cells Transl Med* **6**: 613-621
- Pitcher T, Sousa-Valente J, Malcangio M 2016: The monoiodoacetate model of osteoarthritis pain in the mouse. *J Vis Exp* **111**: 53746
- Samvelyan HJ, Hughes D, Stevens C, Staines KA 2020: Models of osteoarthritis: Relevance and new insights. *Calcif Tissue Int* **109**: 243-256
- Schlichting K, Schell H, Kleemann RU, Schill A, Weiler A, Duda GN, Epari DR 2008: Influence of scaffold stiffness on subchondral bone and subsequent cartilage regeneration in an ovine model of osteochondral defect healing. *Am J Sports Med* **36**: 2379-2391
- Wakitani S, Goto T, Pineda SJ, Young RG, Mansour JM, Caplan AI, Goldberg VM 1994: Mesenchymal cell-based repair of large, full-thickness defects of articular cartilage. *J Bone Joint Surg Am* **76**: 579-592
- Wang M, Shen J, Jin H, Im HJ, Sandy J, Chen D 2011: Recent progress in understanding molecular mechanisms of cartilage degeneration during osteoarthritis. *Ann N Y Acad Sci* **1240**: 61-69
- Zhu W, Guo D, Peng L, Chen YF, Cui J, Xiong J, Lu W, Duan L, Chen K, Zeng Y, Wang D 2017: Repair of rabbit cartilage defect based on the fusion of rabbit bone marrow stromal cells and Nano-HA/PLLA composite material. *Artif Cells Nanomed Biotechnol* **45**: 115-119

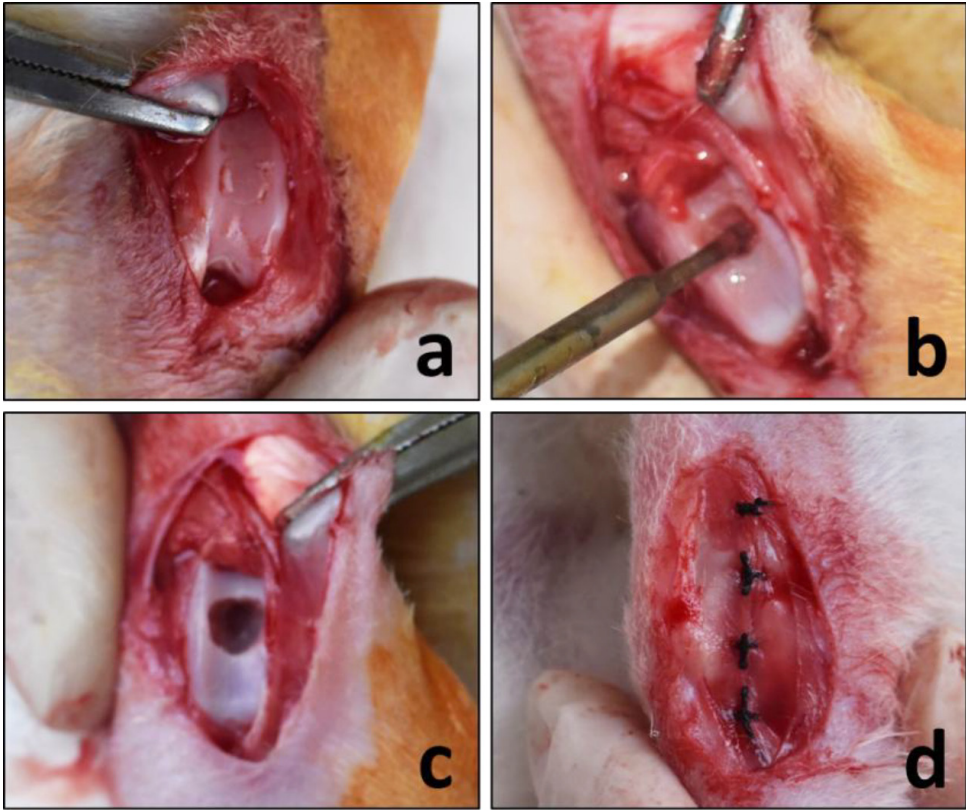


Fig. 1. Surgical procedure for the osteochondral defect in rabbits

a: A longitudinal (parallel to the patellar tendon) incision was made to the skin and sublayers; the patella was dislocated to expose the femoral trochlea; a 3 mm biopsy punch was used to mark the site and the size of the defect on the trochlear groove; b: A dental drill was used to make the defect, the drill site was irrigated with saline; c: A defect of 3 mm in diameter and 3 mm in depth was induced; d: The incision was closed in the order of the joint capsule, muscles, and skin.

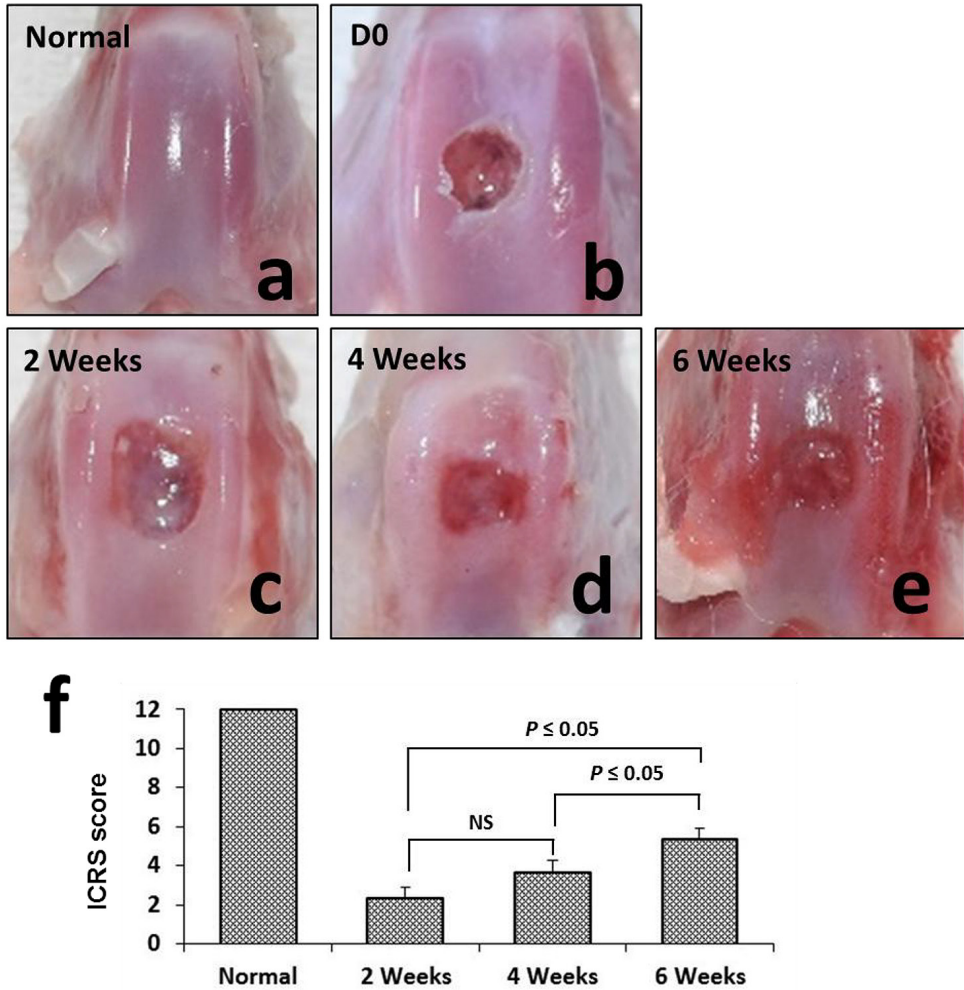


Fig. 2. Macroscopic assessment of the regeneration of osteochondral defects and ICRS score
a: Normal articular cartilage of the rabbit's knee joint; b: The osteochondral defect on the trochlear groove in rabbit knee; c–e: Osteochondral defect repair after 2, 4, and 6 weeks; f: Macroscopic assessment of the repair of osteochondral defects after 2, 4, and 6 weeks according to ICRS scale; NS - non-significant, ICRS - International Cartilage Repair Society.

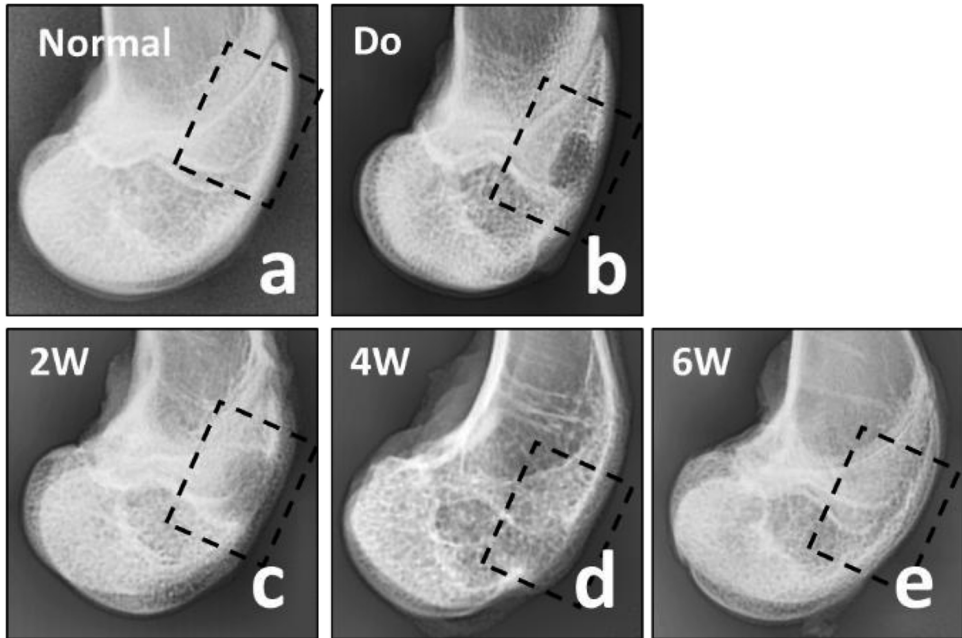


Fig. 3. Assessment of subchondral bone formation by radiography
a: Lateral radiography of normal rabbit femoral head; b: Lateral radiography of the distal end of the rabbit's femur after creating the cleft; c–e: Lateral radiography of the distal end of the rabbit's femur after 2, 4, and 6 weeks of defect induction.

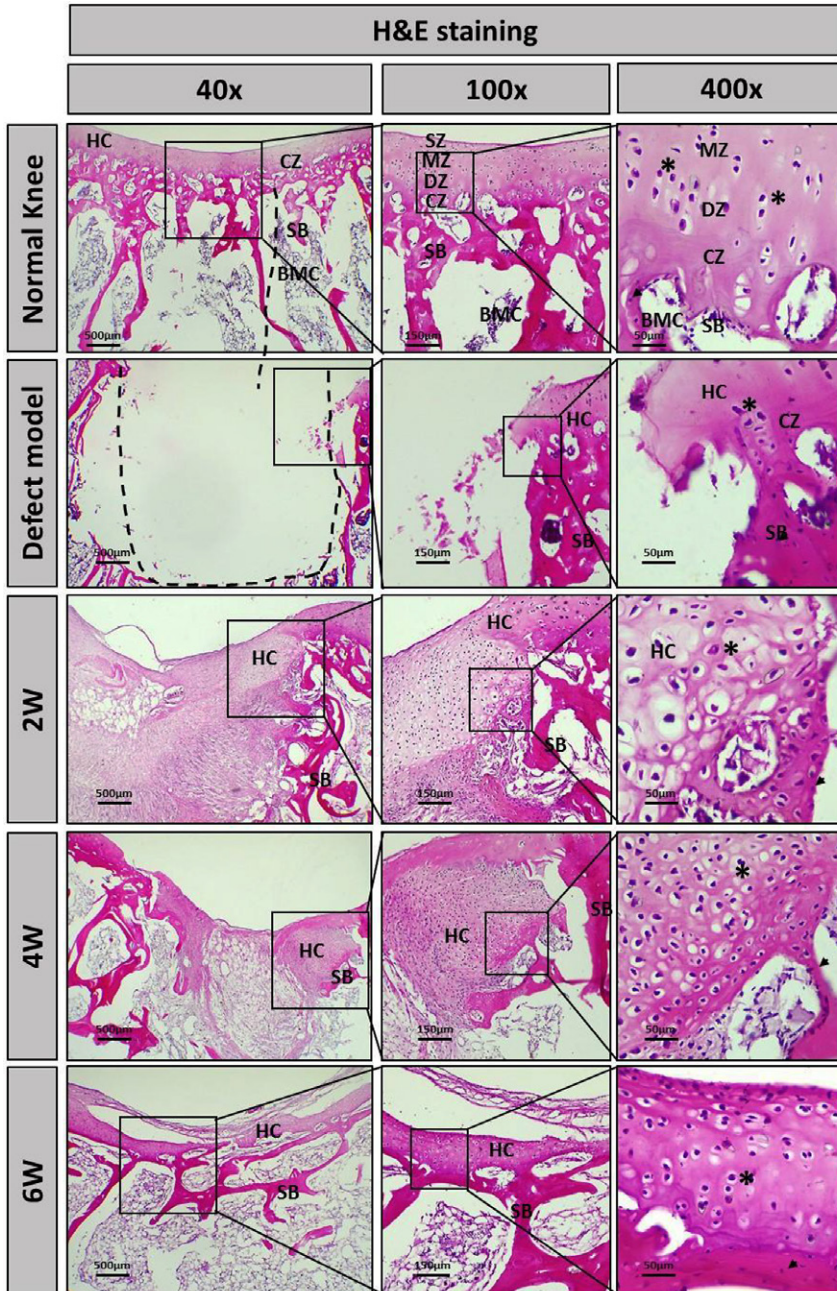


Fig. 4. Histological assessment of osteochondral defect with H&E stain
H&E histological staining images at $\times 40$, 100, and 400 magnification of normal rabbit knee joint tissue, defect model, and reconstruction process after 2, 4, and 6 weeks of surgery. HC - hyaline cartilage; SZ - superficial zone; MZ - middle zone; DZ - deep zone; CZ - calcified zone; SB - subchondral bone; BMC - bone marrow cavity; chondrocytes (asterisk); osteocytes (arrowhead)

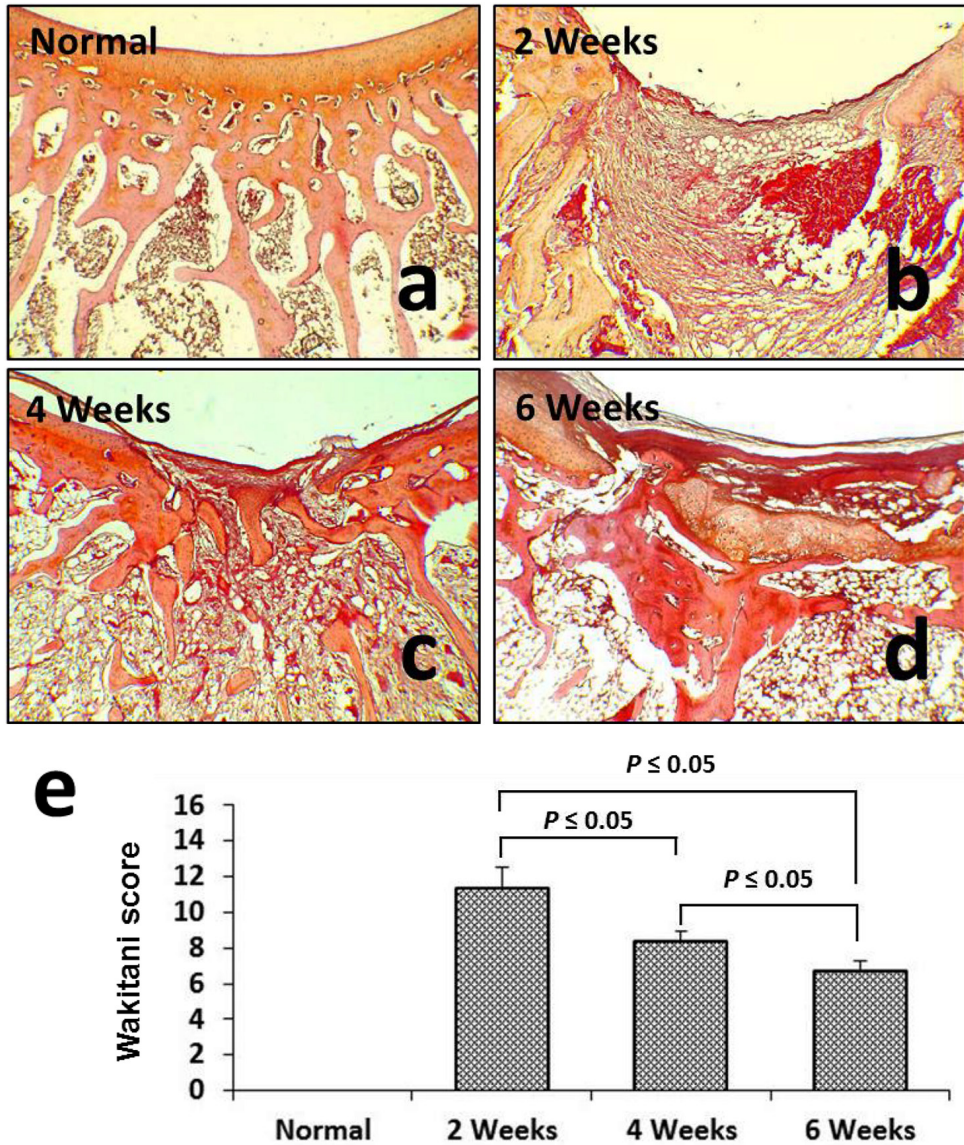


Fig. 5. Histological assessment of osteochondral defect with H&E stain and Wakitani scale
a–d: Safranin O staining of normal rabbit knee cartilage tissue and 2, 4, and 6 weeks after surgery; e: Evaluation of osteochondral regeneration after 2, 4, and 6 weeks of surgery according to Wakitani scale.